CASA: BRIDGING THE GAP BETWEEN POLICY IMPROVEMENT AND POLICY EVALUATION WITH CONFLICT AVERSE POLICY ITERATION

Anonymous authors
Paper under double-blind review

ABSTRACT

We study the problem of model-free reinforcement learning, which is often solved following the principle of Generalized Policy Iteration (GPI). While GPI is typically an interplay between policy evaluation and policy improvement, most conventional model-free methods with function approximation assume the independence of GPI steps, despite of the inherent connections between them. In this paper, we present a method that attempts to eliminate the inconsistency between policy evaluation step and policy improvement step, leading to a conflict averse GPI solution with gradient-based functional approximation. Our method is capital to balancing exploitation and exploration between policy-based and value-based methods and is applicable to existed policy-based and value-based methods. We conduct extensive experiments to study theoretical properties of our method and demonstrate the effectiveness of our method on Atari 200M benchmark.

1 INTRODUCTION

Model-free reinforcement learning has made many impressive breakthroughs in a wide range of Markov Decision Processes (MDP) (Vinyals et al., 2019; Pedersen, 2019; Badia et al., 2020). Overall, the methods could be cast into two categories, value-based methods such as DQN (Mnih et al., 2015) and Rainbow (Hessel et al., 2017), as well as policy-based methods such as TRPO (Schulman et al., 2015a), PPO (Schulman et al., 2017) and IMPALA (Espeholt et al., 2018).

Value-based methods learn state-action values and select the action according to their values. The main target of value-based methods is to approximate the fixed point of the Bellman equation through the generalized policy iteration (GPI) (Sutton & Barto, 2018), which generally consists of policy evaluation and policy improvement. One characteristic of the value-based methods is that unless a more accurate state-action value is estimated by iterations of the policy evaluation, the policy will not be improved. Previous works equip value-based methods with many appropriate designed structures, achieving a more promising sample efficiency (Wang et al., 2016; Schaul et al., 2015; Kapturowski et al., 2018).

Policy-based methods learn a parameterized policy directly without consulting state-action values. One characteristic of policy-based methods is that they incorporate a policy improvement phase in every training step. Conversely, the value-based methods only change the policy when the action corresponding to the highest state-action values is changed. In principle, policy-based methods have a more frequent improvement of policy than value-based methods.

We notice that value-based and policy-based methods locate at the two extremes of GPI, where value-based methods won't improve the policy until a more accurate policy evaluation is achieved, while policy-based methods improve the policy for every training step even when the policy evaluation hasn't converged. To

mitigate the defect of each, we pursuit a technique that is capable of balancing between the two extremes flexibly. We first study the gradients between policy improvement and policy evaluation and notice that they show a positive correlation statistically during the entire training process. To find out if there exists a way that the gradients of the policy improvement and the policy evaluation are parallel, we propose CASA, **C**ritic **AS** an **A**ctor, which theoretically guarantees that the evaluation gradient of the state-action values and the policy gradient to be parallel.

With further delving into the properties of CASA, we find CASA is an innovative combination of value-based and policy-based methods. When the policy-based methods are equipped with CASA, the collapse to the sub-optimal solution as the entropy goes to zero is prevented by the evaluation of the state-action values, which encourages exploration. When the value-based methods are equipped with CASA, the policy improvement via policy gradient is equivalent to the evaluation of the state-action values and a self-bootstrapped policy improvement, which enhances exploitation.

To enable CASA for a large scale off-policy learning, we introduce Doubly-Robust Trace (DR-Trace), which exploits doubly-robust estimator (Jiang & Li, 2016) and guarantees the synchronous convergence of the state-action values and the state values.

Our main contributions are as follows:

(i) We present a novel method CASA which ensures gradient consistency between policy evaluation and policy improvement and present extensive studies on the behavior of the gradients.

(ii) We demonstrate CASA could be freely applied to both policy-based and value-based algorithms with motivating examples.

(iii) We present extensive empirical study on Atari benchmark , where our conflict averse algorithm brings substantial improvements over the baseline methods.

2 PRELIMINARY

Consider an infinite-horizon MDP, defined by a tuple $(\mathcal{S}, \mathcal{A}, p, r, \gamma)$, where $\mathcal{S}$ is the state space, $\mathcal{A}$ is the action space, $p : \mathcal{S} \times \mathcal{A} \times \mathcal{S} \to [0, 1]$ is the state transition probability function, $r : \mathcal{S} \times \mathcal{A} \to \mathbb{R}$ is the reward function, and γ is the discounted factor. The policy is a mapping $\pi : \mathcal{S} \times \mathcal{A} \to [0, 1]$ which assigns a distribution over the action space given a state.

The objective of reinforcement learning is to maximize the *return*, or cumulative discounted rewards,

$$\text{maximize } \mathcal{J} = \mathop{\mathbb{E}}_{s\sim d^\pi}\left[\sum_{k=0}^{\infty} \gamma^k r(s_t, a_t)\right],$$

where $d^\pi(s) = (1-\gamma)\mathbb{E}_\pi[\sum_{k=0}^{\infty} \gamma^k \mathbb{P}(s_k = s)]$ is the stationary distribution induced by π.

Value-based methods maximize $\mathcal{J}$ by estimating various type of value functions: the state value function is defined as $V^\pi(s) = \mathbb{E}_\pi\left[\sum_{k=0}^{\infty} \gamma^k r_k | s\right]$, the state-action value function is defined as $Q^\pi(s, a) = \mathbb{E}_\pi\left[\sum_{k=0}^{\infty} \gamma^k r_k | s, a\right]$; the advantage function is defined as $A^\pi(s, a) = Q^\pi(s, a) - V^\pi(s)$. The objective of maximizing the value functions in value-based methods can be improved through GPI until converging to the optimal policy. For the approximated state-value function Q_θ that estimates Q^π, the policy evaluation is conducted by:

$$\text{minimize } \mathop{\mathbb{E}}_{s\sim d^\pi} \mathop{\mathbb{E}}_{a\sim\pi(\cdot|s)} [(Q^\pi(s, a) - Q_\theta(s, a))^2],$$

where Q^π could be estimated by various methods, e.g., λ-return (Sutton, 1988), GAE (Schulman et al., 2015b), and ReTrace (Munos et al., 2016). The policy improvement is usually achieved by greedily selecting actions with the highest state-action values.

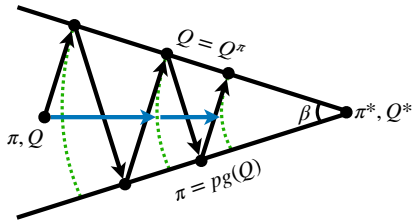

Figure 1: The GPI process in our work. Unlike (Sutton & Barto, 2018), we evaluate π by Q instead of V, and we improve π using policy gradient ascent (pg for brevity) instead of greedy. The learning procedure is shown by the black arrows, i.e., $\mathbf{E} \to \mathbf{I} \to \mathbf{E} \to \mathbf{I} \cdots$.

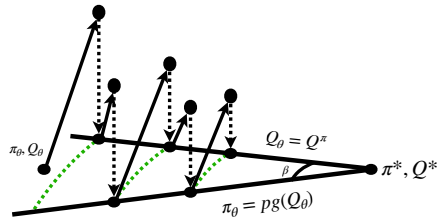

Figure 2: GPI with function approximation. Due to the constraint of approximated function space, the ideal policy iteration cannot be actually achieved. The underlying process of GPI with function approximation can be regarded as doing policy improvement and policy evaluation in an ideal space then being projected back into the approximated function space (Sutton & Barto, 2018; Ghosh et al., 2020).

Policy-based methods maximize $\mathcal{J}$ by optimizing some parameterized policy π_θ according to the policy gradient theorem (Sutton & Barto, 2018),

$$\nabla_\theta \mathcal{J} = \mathop{\mathbb{E}}_{s\sim d^\pi} \mathop{\mathbb{E}}_{a\sim\pi(\cdot|s)} [\Psi(s,a)\nabla_\theta \log \pi_\theta(a|s)],$$

where Ψ is any γ-just function (Schulman et al., 2015b). The vanilla policy gradient theorem uses $\Psi = \sum_{k=0}^{\infty} \gamma^k r_k$. There are also actor-critic algorithms which employs a critic model to approximate $\psi(s,a)$ in the form of baseline, e.g., IMPALA (Espeholt et al., 2018) adopts advantage formulated as $\Psi(s,a) = r + \gamma V^{\tilde{\pi}}(s') - V_\theta(s)$ to update the policy and uses V-Trace to estimate the value $V^{\tilde{\pi}}$.

3 Methodology

3.1 Motivation

For brevity, we abuse the notation and use $\mathbb{E}_\pi$ to represent either $\mathbb{E}_{s\sim d^\pi}\mathbb{E}_{a\sim\pi(\cdot|s)}$ or $\mathbb{E}_{a\sim\pi(\cdot|s)}$ depending on whether $\mathbb{E}_{s\sim d^\pi}$ is needed. We use V_θ to estimate V^π, Q_θ to estimate Q^π and π_θ to represent the policy, where we always use θ to represent all parameters to be optimized. In this work, all estimated values share the same backbone, where most parameters are shared except for individual heads. We use **E** to represent the policy evaluation, which gives the ascent direction of the gradient by $\theta \leftarrow \theta + \eta\mathbb{E}_\pi[(Q^\pi - Q_\theta)\nabla_\theta Q_\theta]$. We use **I** to represent the policy improvement. The policy gradient theorem (Sutton & Barto, 2018) shows that $\nabla_\theta \mathcal{J} = \mathbb{E}_\pi[(Q^\pi - V_\theta)\nabla_\theta \log \pi_\theta]$, so the gradient ascent with **I** is defined as $\theta \leftarrow \theta + \eta\mathbb{E}_\pi[(Q^\pi - V_\theta)\nabla_\theta \log \pi_\theta]$.

Let's recap the GPI process as shown in Figure 1. To get rid of the function approximation error, we first assume the approximation function enjoys infinite capacity. We use $< x, y >$ to denote the angle between two vectors, where $< x, y >= \arccos((x \cdot y)/(||x|| \cdot ||y||))$. We also define an important notion β, which represents the angle between the gradient ascent directions of **I** and **E**, as follows,

$$\beta \stackrel{def}{=} < (Q^\pi - Q_\theta)\nabla_\theta Q_\theta,\ (Q^\pi - V_\theta)\nabla_\theta \log \pi_\theta > .$$

Since $Q^\pi - Q_\theta$ and $Q^\pi - V_\theta$ are two scalars, when $\nabla_\theta Q_\theta \propto \nabla_\theta \log \pi_\theta$, the two sides of β meet. As **I** and **E** are perpendicular to each side of β, they become parallel arrows on opposite directions. The GPI process becomes moving along the meeting sides of β, which is the blue arrow in Figure 1. So there is no conflict between the gradient ascent directions of **I** and **E** anymore except for the step size that is factored by $Q^\pi - Q_\theta$ and $Q^\pi - V_\theta$.

Next, we assume the representation capacity of the approximation function is limited. When the function approximation is involved, i.e. Q^π is estimated by Q_θ and π is approximated by π_θ, from the view of

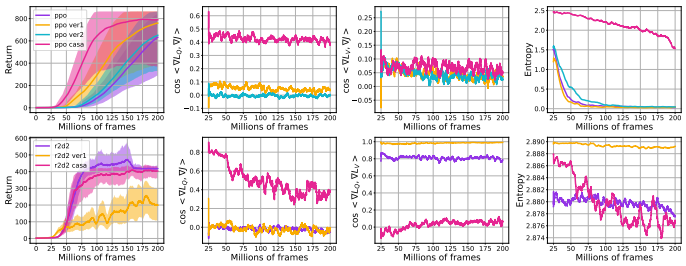

Figure 3: Returns, angles and entropy on Breakout. PPO is adjusted with two additional versions to evaluate state-action values. R2D2 uses a surrogate policy to approximate policy gradient. Entropy of R2D2 is entropy of Boltzmann policy on state-action values. Angles between policy gradient and evaluating state values for PPO, and angles between evaluating state-action values and state values for R2D2 are both positive. Details are in Appendix A.

operators (Ghosh et al., 2020), each of **I** and **E** can be further decomposed into two operators, as shown in Figure 2. One is to do the policy improvement and the policy evaluation, the other is to project into the restricted function space. When $\beta > 0$, GPI with function approximation would involve two projection operators in each iteration, which introduces inevitable approximation error. When $\beta = 0$, if the function approximation error is not considered, we find that the gradient conflict between **I** and **E** would be totally eliminated. If we consider the limitation of the approximation function, similar to the blue arrow in Figure 1, one iteration (represented by two black arrows and two dotted arrows) can be united into one arrow and one dotted arrow (not shown in Figure 2 but analogy to the blue arrow in Figure 1), where the gradient conflict is eliminated and the two projection operators are reduced to one correspondingly.

As stated above, if $\beta = 0$ holds, we can expect that the gradient conflict between the policy improvement and the policy evaluation is eliminated and the function approximation error could be reduced. Note that the importance of $\beta = 0$ has been considered by some earlier works, such as the policy gradient theorem with function approximation (Sutton et al., 1999). Further details on the theorem with notations could be found in Theorem 1 from Appendix A .

To further understand the behavior of β, we track $\cos(\beta)$ of two algorithms PPO and R2D2 as representatives for policy-based and value-based methods, respectively. We show show an important fact in Figure 3 that $\cos(\beta)$ is statistically positive during the entire training process. This is reflected by the fact that cosines of angles between policy gradient and gradient of evaluating state values for PPO are always positive, and cosines of angles between gradients of evaluating state-action values and state values for R2D2 are always positive. It means in the functions approximated by neural networks, the angle between gradient ascent directions of policy improvement and the evaluation are likely to be less then $\pi/2$. More details on this motivating experiment can be found in Appendix A.

The aforementioned conceptual and empirical findings inspire us to raise an important question on GPI: under what condition, the policy improvement and the policy evaluation could share the same ascent direction in their gradients, i.e. $\nabla_\theta Q_\theta \propto \nabla_\theta \log \pi_\theta$?

3.2 Formulation

Denote $\tau \in \mathbb{R}_+$ to be a positive temperature and sg to be a *stop gradient* operator. CASA can estimate V_θ and A_θ by any function parameterized by θ, where π_θ and Q_θ are derived as follows:

$$\begin{cases} \pi_\theta(\cdot|s) = \text{softmax}(A_\theta(s,\cdot)/\tau), \\ \bar{A}_\theta(s,a) = A_\theta(s,a) - \sum_{a'} sg(\pi_\theta(a'|s)) A_\theta(s,a'), \\ Q_\theta(s,a) = \bar{A}_\theta(s,a) + sg(V_\theta(s)). \end{cases} \tag{1}$$

Note that there exist two sg operators in equation 1. The first sg operator is used for computing advantage as $\bar{A}_\theta = A_\theta - \mathbb{E}_\pi[A_\theta] = A_\theta - sg(\pi_\theta) \cdot A_\theta$, where the sg operator here guarantees the gradients between policy improvement and policy evaluation are parallel, which we elaborate later. Intuitively, this sg operator also means that we keep π_θ unchanged when evaluating the policy π_θ. The second sg operator exists in $Q_\theta = \bar{A}_\theta + sg(V_\theta)$. As (Chen & He, 2020) regards sg in siamese representation learning as a case of EM-algorithm (Dempster et al., 1977), a similar interpretation exists here. $Q_\theta = \bar{A}_\theta + sg(V_\theta)$ decomposes the estimation of Q_θ into a two stage problem, where the first is to estimate the advantage of each action without changing the expectation, the second is to estimate the expectation. The equation 1 includes a straightforward refinement of dueling-DQN.

We know dueling-DQN estimates Q_θ by $Q_\theta = A_\theta + V_\theta$, which corresponds to:

$$Q^\pi(s_t, a_t) = \mathbb{E}_p[r_t + \gamma V^\pi(s_{t+1}) - V^\pi(s_t)] + V^\pi(s_t).$$

Since $\mathbb{E}_\pi[\mathbb{E}_p[r_t + \gamma V^\pi(s_{t+1}) - V^\pi(s_t)]] = 0$, we have

$$Q^\pi(s_t, a_t) = \mathbb{E}_p[r_t + \gamma V^\pi(s_{t+1}) - V^\pi(s_t)] - \mathbb{E}_\pi[\mathbb{E}_p[r_t + \gamma V^\pi(s_{t+1}) - V^\pi(s_t)]] + V^\pi(s_t),$$

which is $Q_\theta = A_\theta - \mathbb{E}_\pi[A_\theta] + V_\theta$. This is how we estimates Q_θ in equation 1. This formulation satisfies the necessary condition $\mathbb{E}_\pi[Q_\theta] = V_\theta$ without loss of generality.

3.3 Path Consistency Between Policy Evaluation and Policy Improvement

For brevity, we omit θ and V, Q, A, π are all approximated functions. Denote the estimations of V and Q as $V^{\tilde{\pi}}$ and $Q^{\tilde{\pi}}$ respectively. For instance, one choice is to calculate $V^{\tilde{\pi}}$ and $Q^{\tilde{\pi}}$ by V-Trace (Espeholt et al., 2018) and ReTrace (Munos et al., 2016) respectively.

At training time, the policy evaluation is achieved by updating θ to minimize,

$$L_V(\theta) = \mathbb{E}_\pi[(V^{\tilde{\pi}} - V)^2],\ L_Q(\theta) = \mathbb{E}_\pi[(Q^{\tilde{\pi}} - Q)^2],$$

which gives the ascent direction of θ by:

$$\nabla_\theta L_V(\theta) = \mathbb{E}_\pi\left[(V^{\tilde{\pi}} - V)\nabla_\theta V\right],\ \nabla_\theta L_Q(\theta) = \mathbb{E}_\pi\left[(Q^{\tilde{\pi}} - Q)\nabla_\theta Q\right]. \tag{2}$$

And we make the policy improvement by policy gradient, which gives the ascent direction of θ by:

$$\nabla_\theta \mathcal{J}(\tau, \theta) = \mathbb{E}_\pi\left[\tau(Q^{\tilde{\pi}} - V)\nabla_\theta \log \pi\right], \tag{3}$$

where $\mathcal{J}(\tau, \theta) = \tau\mathbb{E}_\pi[\sum \gamma^t r_t]$. It takes an additional τ, which frees the scale of gradient from τ.

The final gradient ascent direction of θ is given by:

$$\alpha_1 \nabla_\theta L_V + \alpha_2 \nabla_\theta L_Q + \alpha_3 \nabla_\theta \mathcal{J}. \tag{4}$$

With (V, Q, π) defined in equation 1, by Lemma C.1, we have,

$$\nabla_\theta Q = (\mathbf{1} - \pi)\nabla_\theta A = \tau \nabla_\theta \log \pi. \tag{5}$$

For brevity, denote the shared gradient path as $\mathbf{g} = (\mathbf{1} - \pi)\nabla_\theta A$.

Plugging equation 5 into equation 2 equation 3, we have,

$$\nabla_\theta L_Q = \mathbb{E}_\pi\left[(Q^{\tilde{\pi}} - Q)\mathbf{g}\right], \nabla_\theta \mathcal{J} = \mathbb{E}_\pi\left[(Q^{\tilde{\pi}} - V)\mathbf{g}\right]. \tag{6}$$

By equation 6, the directions of the gradients $\mathbf{g}$ are in common. We call it a path. The equation 6 shows that $\nabla_\theta L_Q$ and $\nabla_\theta \mathcal{J}$ walk along the same path $\mathbf{g}$. The difference is that $\nabla_\theta L_Q$ walks with step size $Q^{\tilde{\pi}} - Q$, but $\nabla_\theta \mathcal{J}$ walks with step size $Q^{\tilde{\pi}} - V$. When we share all variables to estimate Q and π, except for τ, this is

exactly the case $\beta = 0$ in Figure 1. Under such condition, there is no gradient conflict between the policy improvement and the policy evaluation. This is why we call it **C**ritic **AS** an **A**ctor.

If we make a subtraction between $\nabla_\theta L_Q$ and $\nabla_\theta \mathcal{J}$, we have,

$$\nabla_\theta \mathcal{J} = \nabla_\theta L_Q + \mathbb{E}_\pi \left[(Q - V)\mathbf{g}\right]. \tag{7}$$

We know $\mathbb{E}_\pi \left[(Q - V)\mathbf{g}\right]$ is a self-bootstrapped policy gradient with function approximated Q. If we regard $Q^{\tilde{\pi}}$ as a *better* estimation of the ground truth state-action values than Q, the equation 7 says that the policy improvement equals to the policy evaluation plus a *worse* policy improvement, where the *worse* policy improvement entirely depends on the evaluated values. Recalling the fact that the value-based methods improves the policy by greedily selecting actions according to Q, if we apply $\nabla_\theta \mathcal{J}$ on θ, it additionally utilizes Q to do policy improvement. This is a more greedy usage of Q to improve policy than its usual usage.

If we exploit the structural information as (V, Q, π) defined by equation 1, by Lemma C.2,

$$\mathbb{E}_\pi \left[(Q - V)\mathbf{g}\right] = \tau \mathbb{E}_\pi \left[(Q - V)\nabla_\theta \log \pi\right] = -\tau^2 \nabla_\theta \mathbf{H}[\pi],$$

then we have,

$$\nabla_\theta L_Q = \nabla_\theta \mathcal{J} + \tau^2 \nabla_\theta \mathbf{H}[\pi]. \tag{8}$$

The equation 8 shows $\nabla_\theta L_Q$ is a policy gradient with an entropy regularization. If we apply $\nabla_\theta L_Q$ on θ for policy-based methods, an entropy regularization works implicitly by $\alpha_2 \nabla_\theta L_Q$ in equation 4, which prevents the policy collapse to a sub-optimal solution. An intuitive explanation is that, as Q and π share A, but the target of Q is dominated by MDP, so Q regularizes A to prevent π from collapse to sub-optimal solutions.

3.4 DR-Trace and Off-Policy Training

	DR-Trace	V-Trace / ReTrace
	$\delta_t^{DR} = r_t + \gamma V(s_{t+1}) - Q(s_t, a_t)$	$\delta_t^{V/Q} = r_t + \gamma V(s_{t+1})/Q(s_{t+1}, a_{t+1}) - V(s_t)/Q(s_t, a_t)$
$V^{\tilde{\pi}}$	$\mathbb{E}_\mu[V_t + \sum_{k\geq 0} \gamma^k c_{[t:t+k-1]} \rho_{t+k} \delta_{t+k}^{DR}]$	$\mathbb{E}_\mu[V_t + \sum_{k\geq 0} \gamma^k c_{[t:t+k-1]} \rho_{t+k} \delta_{t+k}^{V}]$
$Q^{\tilde{\pi}}$	$\mathbb{E}_\mu[Q_t + \sum_{k\geq 0} \gamma^k c_{[t+1:t+k-1]} (1_{\{k=0\}} + 1_{\{k>0\}} \rho_{t+k}) \delta_{t+k}^{DR}]$	$\mathbb{E}_\mu[Q_t + \sum_{k\geq 0} \gamma^k c_{[t+1:t+k]} \delta_{t+k}^{Q}]$
$\nabla \mathcal{J}$	$\mathbb{E}_\mu[\rho_t (Q_t^{\tilde{\pi}} - V_t) \nabla \log \pi]$	$\mathbb{E}_\mu[\rho_t (r_t + V_{t+1}^{\tilde{\pi}} - V_t) \nabla \log \pi]$

Table 1: Comparison between DR-Trace and V-Trace/ReTrace.

To enable off-policy training, one choice is to estimate $V^{\tilde{\pi}}$ and $Q^{\tilde{\pi}}$ in equation 2 and equation 3 by V-Trace and ReTrace. As CASA estimates (V, Q, π) simultaneously, we notice that applying Doubly Robust (Jiang & Li, 2016) is feasible and suitable. It's natural to propose DR-Trace. We find the convergence rate and the fixed point of DR-Trace are the same as V-Trace's according to its convergence proof. For completeness, we provide DR-Trace and its comparison with V-Trace/ReTrace in Table 1. More details are in Appendix B.

4 Experiments

4.1 Basic Setup

We employ a Learner-Actor pipeline (Espeholt et al., 2018) for large-scale training. To deal with partially observable MDP (POMDP), we use a recurrent encoder by LSTM (Schmidhuber, 1997) with 256 units. All estimated values share the same backbone, which is followed by two fully connected layers for each individual head. We use *burn-in* (Kapturowski et al., 2018) to deal with representational drift. We use no intrinsic reward and no entropy regularization in any experiment. We find that using life information can greatly increase the performance of some games. However, to be general, we will not end the episode if life is lost. All hyperparameters are in Appendix D.

	PPO		PPO+CASA	R2D2		R2D2+CASA
Func. Approx.	$(V, logit) = (V_\theta, logit_\theta)$ $\pi = \text{softmax}(logit)$	$\Rightarrow$	$(V, A) = (V_\theta, A_\theta)$ $\pi = \text{softmax}(A/\tau)$ $\bar{A} = A - sg(\pi) \cdot A$ $Q = \bar{A} + sg(V)$	$(V, A) = (V_\theta, A_\theta)$ $Q = A + V$	$\Rightarrow$	$(V, A) = (V_\theta, A_\theta)$ $\pi = \text{softmax}(A/\tau)$ $\bar{A} = A - sg(\pi) \cdot A$ $Q = \bar{A} + sg(V)$
Gradient	$0.5\nabla L_V + \nabla \mathcal{J}$	$\Rightarrow$	$0.5\nabla L_V + \nabla L_Q + \nabla \mathcal{J}$	∇L_Q	$\Rightarrow$	$0.5\nabla L_V + \nabla L_Q + \nabla \mathcal{J}$

Table 2: Examples of applying CASA on policy-based methods (PPO) and value-based methods (R2D2).

4.2 Application of CASA on Representative Algorithms

CASA is applicable to existing algorithms. We take PPO and R2D2 for demonstration. The application of CASA on PPO is straightforward. Applying CASA on R2D2 is impossible as either ϵ-greedy policy or $\arg\max Q$ policy breaks the gradient. This problem is the same as calculating the gradients of policy improvement for value-based methods. We use a surrogate policy $\pi_{surrogate} = \text{softmax}(A/\tau)$, which is discussed in Appendix A. Table 2 summarizes adjustments of function approximations and training gradients.

It's noticeable that PPO+CASA and R2D2+CASA have the same function approximation. Recalling the fact that value-based methods improve the policy when a more accurate evaluation is achieved and policy-based methods improve the policy for every step, we can balance the two flexibly without any gradient conflict by adjusting $\alpha_1, \alpha_2, \alpha_3$ in equation 4.

In Figure 3, algorithms with CASA show much higher $\cos(\beta)$. PPO+CASA does more exploration than the original PPO, as the entropy of π doesn't easily drop to zero. R2D2+CASA tends to distinct the state-action values, where we use the entropy of Q to measure how greedy the current state-action values are. We also include more angles that are interesting in Appendix A.

4.3 Behavior of Gradients on different structures

Though we show that CASA satisfies $\nabla Q \propto \nabla \log \pi$, which means $\beta = 0$, it's unknown if the structure of CASA is unique. As $Q = A - \mathbb{E}_\pi[A] + sg(V)$ is a direct refinement of dueling-Q, we try several different structures of PPO+CASA within three categories. All settings of estimating state-action values are shown in Table 3. We always use $0.5 \cdot \nabla L_V + \nabla L_Q + \nabla \mathcal{J}$ as the training gradient. We present Breakout and Qbert in Figure 4. We observes cosines of four different angle of all structures, which include $< \nabla Q, \nabla \log \pi >$ and angles between ∇L_V, ∇L_Q and $\nabla \mathcal{J}$.

For the sake of clarity, we group PPO+CASA and type 3 as sg-V group, type 2 and type 4 as no-sg-V group. The sg-V group has higher $< \nabla Q, \nabla \log \pi >$ and higher $< \nabla L_Q, \nabla \mathcal{J} >$, which is more close to the assumption of Theorem 1. The no-sg-V group has higher $< \nabla L_Q, \nabla L_V >$, which is simple to explain as the gradient of Q also includes the gradient of V. However, this seems to be hard for distinguishing state-action values, as no-sg-V group is always worst than its contrast in sg-V group.

PPO+CASA	$Q = A_\theta - sg(\pi_\theta) \cdot A_\theta + sg(V_\theta)$
type 1	$Q = A_\theta - \pi_\theta \cdot A_\theta + sg(V_\theta)$
type 2	$Q = A_\theta - sg(\pi_\theta) \cdot A_\theta + V_\theta$
type 3	$Q = A_\theta + sg(V_\theta)$
type 4	$Q = A_\theta + V_\theta$
type 5	$Q = Q_\theta$

Table 3: Behavior gradient types. Type 1&2 are CASA-like structures, where type 1 removes sg of π and type 2 removes sg of V_θ. Type 3&4 are dueling-like structures, where type 3 adds sg to V for dueling-Q and type 4 is dueling-Q. Type 5 uses a new head to estimate Q_θ separately, which can be considered as an auxiliary task to estimate Q^π.

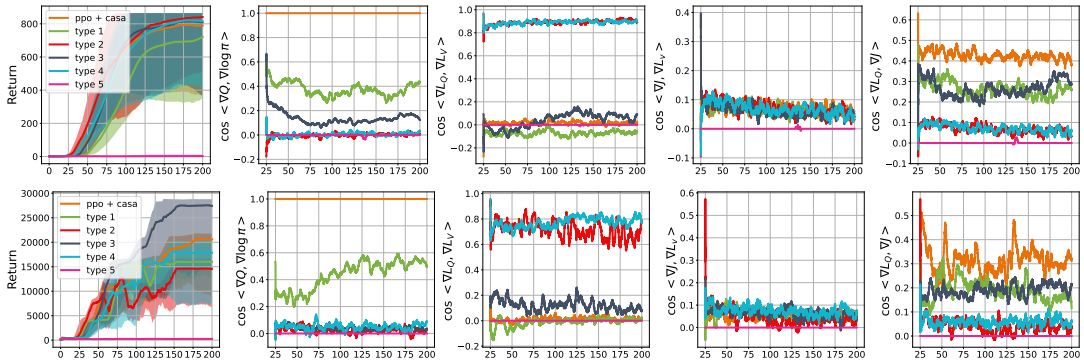

Figure 4: The ablation results evaluated on Breakout (top row) and Qbert (bottom row). From left to right is the *return* curve, the *angle between the gradient of log policy and the gradient of Q function*, and the *angle between the gradients of different losses*.

PPO+CASA has $\cos < \nabla Q, \nabla \log \pi >= 1$ and the highest $\beta = \cos < \nabla L_Q, \nabla \mathcal{J} >$ as expected. We find type 1 is less satisfied in angles and has less returns than PPO+CASA. Hence, when applying a CASA-like structure, CASA is superior to type 1.

Type 5 only adds an auxiliary task of estimating Q^π by Q_θ via ∇L_Q, but surprisingly fails learning in all games. It reflects the fact that even the gradient from an explainable auxiliary target function can cause great failure. It's surprising to see that cosines of all four angles of type 5 are very close to zero. One can explain this as all gradients are pulling each other, but this is far from satisfactory. This phenomenon shows a potential condition to decide what a good auxiliary task may be.

4.4 Evaluation of CASA on Atari Games

	Mean HNS	Median HNS	Mean SABER	Median SABER
Rainbow	873.97	230.99	28.39	4.92
IMPALA	957.34	191.82	29.45	4.31
LASER	1741.36	**454.91**	**36.77**	8.08
CASA	**1941.08**	246.36	36.10	**10.29**

Table 4: Evaluation scores for the methods on Atari benchmark presented in %.

We present an extensive evaluation on CASA, where we train CASA + DR-Trace on 57 Atari games and report the results in terms of two metrics. The first is Human Normalized Score (HNS), which normalizes the reward by random policy and human expert policies. The other is Standardized Atari BEnchmark for RL (SABER), which normalizes the reward by random policy and human world records, where the normalized score is capped by 200%. SABER is considered because recent studies show that the median HNS could easily get hacked by the algorithm since it is sensitive to improvement on a small subset of games. Compared to HNS, SABER adopts higher human scores and clips the scores. Table 4 summarizes the results. Note that CASA is a variant of IMPALA with DR-Trace, and it achieves substantially better records than IMPALA across all the evaluation metrics. It also scores substantially better than all the methods in terms of mean HNS and median SABER scores. Though off-policy methods are known as privileged for HNS evaluation due to replay, CASA could outperform strong off-policy baseline Rainbow. Though LASER could outperform CASA in Median HNS and Mean SABER, CASA outperforms it on the other two metrics of median SABER and mean HNS.

Overall, the aforementioned results demonstrate the conflict-averse strategy in CASA efficiently boosts the performance in large-scale training scenarios and outperform strong on/off-policy algorithms. Details on the hyperparameters and individual games are presented in Appendix D and Appendix E, respectively.

5 Related Works

Both value-based or policy-based approaches comply with the principle of GPI. Value-based methods update the value functions for policy evaluation followed by a simple practice of policy improvement in the greedy form, whereas policy-based methods improve the policy progressively with intermediate value functions. Thus, for both value-based and policy-based strands, the two GPI steps are coarsely related to each other such that jointly optimizing both functions might potentially bring conflicts. Despite of such crucial issue in GPI with function approximation, most decent model-free algorithms adopt a standard policy improvement/evaluation regime without considering conflict diminishing properties. The issue of reducing conflicts among multiple models trained simultaneously was considered in earlier machine learning literature, such as for robust parameter estimation for multiple estimators under incomplete data (Robins & Rotnitzky, 1995; Lunceford & Davidian, 2004; Kang & Schafer, 2007) and multitask learning with gradient similarity measure (Chen et al., 2020; Yu et al., 2020; Javaloy & Valera, 2022).

When the idea is introduced to reinforcement learning, earliest attempts tackle conservative and safe policy iteration problems (Kakade & Langford, 2002; Hazan & Kale, 2011; Pirotta et al., 2013). Recently, more works have emerged to study GPI in a fine-grained manner. In (Ghosh et al., 2020), a new Bellman operator is introduced which implements GPI with a policy improvement operator and a projection operator, where the projection attempts to find the best approximation of policy among realizable policies. In (Raileanu & Fergus, 2021), the policy and value updates are decoupled by approximating two networks with representation regularization. In (Cobbe et al., 2021), GPI is separated into a policy improvement and a feature distillation step. On contrast to the aforementioned works, we tackle the conflicts in GPI at the gradient-level, with theoretical analysis. Our work is mostly related to (Nachum et al., 2017), which utilizes both the unbiasedness and stability of on-policy training and the data efficiency of off-policy training to form a soft consistency error. Our work bridges the gap between the two GPI steps from an alternative angle of establishing a closer relationship between policy and value functions in their forms, without the focus on off-policy correction.

6 Ethics and Reproducibility Statement

This paper is aimed at academic issues in deep reinforcement learning, and the experiment used is also in the early stage, but it may provide opportunities for malicious applications of reinforcement learning in the future. We describe all details to reproduce the main experimental results in Appendix D.

7 Conclusion

This paper proposes a novel method to resolve the inconsistency between policy improvement and policy evaluation steps in GPI with a unified gradient-based attempt. To this end, we propose an innovative actor-critic design termed **C**ritic **AS** an **A**ctor (CASA) which consolidates the policy improvement and policy evaluation with a more guaranteed policy improvement. We present both sophisticated theoretical proof as well as empirical evaluation for CASA on large-scale policy training domains. The results show that our proposed method could achieve state-of-the-art performance standards with noticeable performance gain over several strong baselines when evaluated on ALE 200 million (200M) benchmark. We also present several ablation studies, which demonstrates the effectiveness of the proposed method's theoretical properties. Future work includes integrating CASA with more policy-based and value-based policy training algorithms and studying alternative properties of GPI to further improve the consistency.

REFERENCES

Adrià Puigdomènech Badia, Bilal Piot, Steven Kapturowski, Pablo Sprechmann, Alex Vitvitskyi, Daniel Guo, and Charles Blundell. Agent57: Outperforming the atari human benchmark. *arXiv preprint arXiv:2003.13350*, 2020.

Xinlei Chen and Kaiming He. Exploring simple siamese representation learning. *arXiv preprint arXiv:2011.10566*, 2020.

Zhao Chen, Jiquan Ngiam, Yanping Huang, Thang Luong, Henrik Kretzschmar, Yuning Chai, and Dragomir Anguelov. Just pick a sign: Optimizing deep multitask models with gradient sign dropout. In *Advances in Neural Information Processing Systems 33: Annual Conference on Neural Information Processing Systems 2020, NeurIPS 2020, December 6-12, 2020, virtual*, 2020.

Karl Cobbe, Jacob Hilton, Oleg Klimov, and John Schulman. Phasic policy gradient. In *Proceedings of the 38th International Conference on Machine Learning, ICML 2021, 18-24 July 2021, Virtual Event*, volume 139 of *Proceedings of Machine Learning Research*, pp. 2020–2027, 2021.

A. P. Dempster, N. M. Laird, and D. B. Rubin. Maximum likelihood from incomplete data via the em algorithm. *JOURNAL OF THE ROYAL STATISTICAL SOCIETY, SERIES B*, 39(1):1–38, 1977.

Lasse Espeholt, Hubert Soyer, Remi Munos, Karen Simonyan, Volodymir Mnih, Tom Ward, Yotam Doron, Vlad Firoiu, Tim Harley, Iain Dunning, et al. Impala: Scalable distributed deep-rl with importance weighted actor-learner architectures. *arXiv preprint arXiv:1802.01561*, 2018.

Dibya Ghosh, Marlos C Machado, and Nicolas Le Roux. An operator view of policy gradient methods. *Advances in Neural Information Processing Systems*, 33:3397–3406, 2020.

Elad Hazan and Satyen Kale. Better algorithms for benign bandits. *J. Mach. Learn. Res.*, 12:1287–1311, 2011.

Matteo Hessel, Joseph Modayil, Hado Van Hasselt, Tom Schaul, Georg Ostrovski, Will Dabney, Dan Horgan, Bilal Piot, Mohammad Azar, and David Silver. Rainbow: Combining improvements in deep reinforcement learning. *arXiv preprint arXiv:1710.02298*, 2017.

Adrián Javaloy and Isabel Valera. Rotograd: Gradient homogenization in multitask learning. In *The Tenth International Conference on Learning Representations, ICLR 2022, Virtual Event, April 25-29, 2022*, 2022.

Nan Jiang and Lihong Li. Doubly robust off-policy value evaluation for reinforcement learning. In *International Conference on Machine Learning*, pp. 652–661. PMLR, 2016.

Sham M. Kakade and John Langford. Approximately optimal approximate reinforcement learning. In *Machine Learning, Proceedings of the Nineteenth International Conference (ICML 2002), University of New South Wales, Sydney, Australia, July 8-12, 2002*, pp. 267–274, 2002.

Joseph DY Kang and Joseph L Schafer. Demystifying double robustness: A comparison of alternative strategies for estimating a population mean from incomplete data. *Statistical science*, 22(4):523–539, 2007.

Steven Kapturowski, Georg Ostrovski, John Quan, Remi Munos, and Will Dabney. Recurrent experience replay in distributed reinforcement learning. In *International conference on learning representations*, 2018.

Jared K Lunceford and Marie Davidian. Stratification and weighting via the propensity score in estimation of causal treatment effects: a comparative study. *Statistics in medicine*, 23(19):2937–2960, 2004.

Volodymyr Mnih, Koray Kavukcuoglu, David Silver, Andrei A Rusu, Joel Veness, Marc G Bellemare, Alex Graves, Martin Riedmiller, Andreas K Fidjeland, Georg Ostrovski, et al. Human-level control through deep reinforcement learning. *nature*, 518(7540):529–533, 2015.

Remi Munos, Tom Stepleton, Anna Harutyunyan, and Marc Bellemare. Safe and efficient off-policy reinforcement learning. In D. D. Lee, M. Sugiyama, U. V. Luxburg, I. Guyon, and R. Garnett (eds.), *Advances in Neural Information Processing Systems 29*, pp. 1054–1062. Curran Associates, Inc., 2016.

Ofir Nachum, Mohammad Norouzi, Kelvin Xu, and Dale Schuurmans. Bridging the gap between value and policy based reinforcement learning. In *Advances in Neural Information Processing Systems*, pp. 2775–2785, 2017.

Carsten Lund Pedersen. Re: Human-level performance in 3d multiplayer games with population-based reinforcement learning. *Science*, 2019.

Matteo Pirotta, Marcello Restelli, Alessio Pecorino, and Daniele Calandriello. Safe policy iteration. In *Proceedings of the 30th International Conference on Machine Learning, ICML 2013, Atlanta, GA, USA, 16-21 June 2013*, volume 28 of *JMLR Workshop and Conference Proceedings*, pp. 307–315, 2013.

Roberta Raileanu and Rob Fergus. Decoupling value and policy for generalization in reinforcement learning. In *Proceedings of the 38th International Conference on Machine Learning, ICML 2021, 18-24 July 2021, Virtual Event*, volume 139 of *Proceedings of Machine Learning Research*, pp. 8787–8798, 2021.

James M Robins and Andrea Rotnitzky. Semiparametric efficiency in multivariate regression models with missing data. *Journal of the American Statistical Association*, 90(429):122–129, 1995.

Tom Schaul, John Quan, Ioannis Antonoglou, and David Silver. Prioritized experience replay. *arXiv preprint arXiv:1511.05952*, 2015.

Sepp Hochreiter; Jürgen Schmidhuber. Long short-term memory. *Neural Computation.*, 1997.

Simon Schmitt, Matteo Hessel, and Karen Simonyan. Off-policy actor-critic with shared experience replay. In *International Conference on Machine Learning*, pp. 8545–8554. PMLR, 2020.

John Schulman, Sergey Levine, Pieter Abbeel, Michael Jordan, and Philipp Moritz. Trust region policy optimization. In *International conference on machine learning*, pp. 1889–1897, 2015a.

John Schulman, Philipp Moritz, Sergey Levine, Michael Jordan, and Pieter Abbeel. High-dimensional continuous control using generalized advantage estimation. *arXiv preprint arXiv:1506.02438*, 2015b.

John Schulman, Filip Wolski, Prafulla Dhariwal, Alec Radford, and Oleg Klimov. Proximal policy optimization algorithms. *arXiv preprint arXiv:1707.06347*, 2017.

Richard S. Sutton. Learning to predict by the methods of temporal differences. *Mach. Learn.*, 3:9–44, 1988.

Richard S Sutton and Andrew G Barto. *Reinforcement learning: An introduction*. MIT press, 2018.

Richard S Sutton, David McAllester, Satinder Singh, and Yishay Mansour. Policy gradient methods for reinforcement learning with function approximation. *Advances in neural information processing systems*, 12, 1999.

Marin Toromanoff, Emilie Wirbel, and Fabien Moutarde. Is deep reinforcement learning really superhuman on atari? leveling the playing field. *arXiv preprint arXiv:1908.04683*, 2019.

Oriol Vinyals, Igor Babuschkin, Wojciech M Czarnecki, Michaël Mathieu, Andrew Dudzik, Junyoung Chung, David H Choi, Richard Powell, Timo Ewalds, Petko Georgiev, et al. Grandmaster level in starcraft ii using multi-agent reinforcement learning. *Nature*, 575(7782):350–354, 2019.

Ziyu Wang, Tom Schaul, Matteo Hessel, Hado Hasselt, Marc Lanctot, and Nando Freitas. Dueling network architectures for deep reinforcement learning. In *International conference on machine learning*, pp. 1995–2003, 2016.

Tianhe Yu, Saurabh Kumar, Abhishek Gupta, Sergey Levine, Karol Hausman, and Chelsea Finn. Gradient surgery for multi-task learning. In *Advances in Neural Information Processing Systems 33: Annual Conference on Neural Information Processing Systems 2020, NeurIPS 2020, December 6-12, 2020, virtual*, 2020.

A GRADIENTS BETWEEN POLICY IMPROVEMENT AND POLICY EVALUATION

Theorem 1 (Sutton et al. (1999)). *If Q_θ satisfies $\mathbb{E}_\pi[(Q^\pi - Q_\theta)\nabla_\theta Q_\theta] = 0$ and $\nabla_\theta Q_\theta = \nabla_\theta \log \pi_\theta$, then we have*

$$\nabla_\theta \mathcal{J} = \mathbb{E}_\pi[Q_\theta \nabla_\theta \log \pi_\theta].$$

	Function Approximation	Train Gradients	Interested Angles
PPO	$(V, logit) = (V_\theta, logit_\theta)$ $\pi = \text{softmax}(logit)$	$0.5\nabla L_V + \nabla \mathcal{J}$	$< \nabla L_V, \nabla \mathcal{J} >$
PPO ver.1	$(Q, logit) = (Q_\theta, logit_\theta)$, $\pi = \text{softmax}(logit)$ $V = sg(\pi) \cdot Q$	$0.5\nabla L_V + \nabla \mathcal{J}$	$< \nabla L_V, \nabla \mathcal{J} >$ $< \nabla L_Q, \nabla \mathcal{J} >$ $< \nabla L_V, \nabla L_Q >$ $< \nabla Q, \nabla \log \pi >$
PPO ver.2	$(Q, logit) = (Q_\theta, logit_\theta)$, $pi = \text{softmax}(logit)$ $V = sg(\pi) \cdot Q$	$0.5\nabla L_V + \nabla L_Q + \nabla \mathcal{J}$	$< \nabla L_V, \nabla \mathcal{J} >$ $< \nabla L_Q, \nabla \mathcal{J} >$ $< \nabla L_V, \nabla L_Q >$ $< \nabla Q, \nabla \log \pi >$
PPO+CASA	$(V, A) = (V_\theta, A_\theta)$, $\pi = \text{softmax}(A/\tau)$, $\bar{A} = A - sg(\pi) \cdot A$ $Q = \bar{A} + sg(V)$	$0.5\nabla L_V + \nabla L_Q + \nabla \mathcal{J}$	$< \nabla L_V, \nabla \mathcal{J} >$ $< \nabla L_Q, \nabla \mathcal{J} >$ $< \nabla L_V, \nabla L_Q >$ $< \nabla Q, \nabla \log \pi >$

Table 5: PPO is the original PPO. PPO ver.1 and PPO ver.2 are adapted versions to calculate ∇L_Q. PPO+CASA is applying CASA on PPO, which is described in Sec. 4.2.

	Function Approximation	Train Gradients	Interested Angles
R2D2	$(V, A) = (V_\theta, A_\theta)$ $Q = A + V$ $\pi = \text{softmax}(A/\tau)$	∇L_Q	$< \nabla L_V, \nabla \mathcal{J} >$ $< \nabla L_Q, \nabla \mathcal{J} >$ $< \nabla L_V, \nabla L_Q >$
R2D2 ver.1	$(V, A) = (V_\theta, A_\theta)$ $Q = A + V$ $\pi = \text{softmax}(A/\tau)$	$0.5\nabla L_V + \nabla L_Q$	$< \nabla L_V, \nabla \mathcal{J} >$ $< \nabla L_Q, \nabla \mathcal{J} >$ $< \nabla L_V, \nabla L_Q >$
R2D2+CASA	$(V, A) = (V_\theta, A_\theta)$, $\pi = \text{softmax}(A/\tau)$, $\bar{A} = A - sg(\pi) \cdot A$ $Q = \bar{A} + sg(V)$	$0.5\nabla L_V + \nabla L_Q + \nabla \mathcal{J}$	$< \nabla L_V, \nabla \mathcal{J} >$ $< \nabla L_Q, \nabla \mathcal{J} >$ $< \nabla L_V, \nabla L_Q >$

Table 6: R2D2 is the original R2D2. R2D2 ver.1 is adapted version to include ∇L_V for training. R2D2+CASA is applying CASA on R2D2, which is described in Sec. 4.2.

To understand the behavior of

$$\beta =< (Q^\pi - Q_\theta)\nabla_\theta Q_\theta,\ (Q^\pi - V_\theta)\nabla_\theta \log \pi_\theta >$$

in reinforcement learning algorithms, we choose PPO as a representative as policy-based methods and R2D2 as a representative as value-based algorithms.

Define

$$L_V(\theta) = \mathbb{E}_\pi[(V^\pi - V_\theta)^2],\ L_Q(\theta) = \mathbb{E}_\pi[(Q^\pi - Q_\theta)^2],$$

and

$$\nabla_\theta \mathcal{J}(\theta) = \mathbb{E}_\pi\left[(Q^\pi - V_\theta)\nabla_\theta \log \pi\right].$$

We usually have above three kinds of loss functions in reinforcement learning, which aim to estimate the state values, state-action values and the policy. We do not talk about the estimations of V^π and Q^π as they are estimated as their usual way of PPO's and R2D2's. All hyperparameters are listed in Appendix D.

The fact that PPO only has $\nabla_\theta L_V$ and $\nabla_\theta \mathcal{J}$ and R2D2 only has $\nabla_\theta L_Q$ is the main difficulty to track both the gradients of policy improvement and policy evaluation. To solve the problem, we adjust PPO and R2D2 with different versions.

For PPO, we displace the estimation of V_θ by $sg(\pi) \cdot Q_\theta$, where Q_θ is estimated by function approximation and V is estimated by taking the expectation of Q_θ. All versions of PPO are listed in Table 5.

For R2D2, we point out that though we apply ϵ-greedy to interact with environments, ϵ is only used for exploration and the final target policy of value-based methods is simply $\arg\max Q_\theta$. Because $\arg\max Q_\theta$ breaks the gradient, we use a surrogate policy to approximate the gradient of policy improvement. Since R2D2 uses dueling structure and $\text{softmax}(A_\theta/\tau) = \text{softmax}(Q_\theta/\tau) \overset{\tau\to 0+}{\longrightarrow} \arg\max Q_\theta$, we use $\pi_{surrogate} = \text{softmax}(A_\theta/\tau)$ to calculate the policy gradient. We only use $\pi_{surrogate}$ on learner to calculate the gradient, the policy that interacts with environments is still ϵ-greedy. All versions of R2D2 are listed in Table 6.

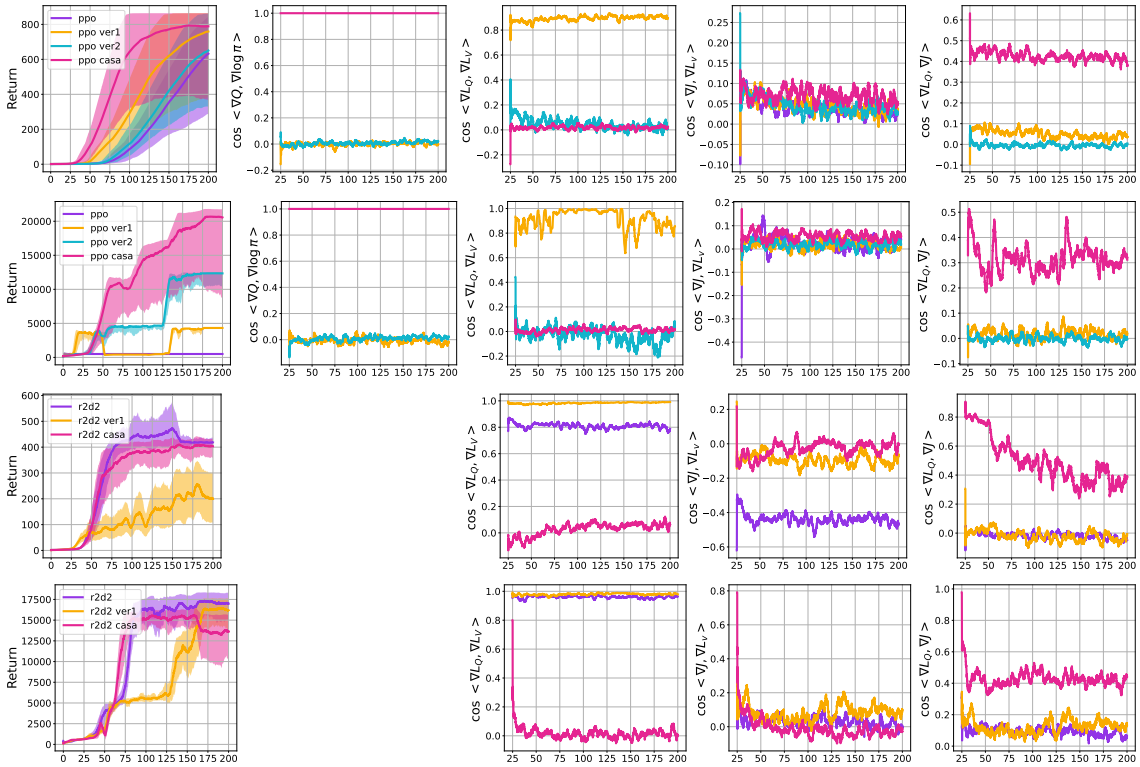

Figure 5: Angles of Gradients and Returns of versions of PPO and R2D2 defined in Table 5 and Table 6.

B DR-TRACE

As CASA estimates (V, Q, π), we would ask **i)** how to guarantee that $\tilde{\pi}_{VTrace} = \tilde{\pi}_{ReTrace}$, **ii)** how to exploit (V, Q, π) to make a better estimation. Though we can apply V-Trace to estimate V and ReTrace to estimate Q with proper hyperparameters to guarantee $\tilde{\pi}_{VTrace} = \tilde{\pi}_{ReTrace}$, it's more reasonable to estimate (V, Q) together. Inspired by Doubly Robust, which is shown to maximally reduce the variance, we introduce DR-Trace, which estimates V by

$$V_{DR}^{\tilde{\pi}}(s_t) \overset{def}{=} \mathbb{E}_\mu[V(s_t) + \sum_{k\geq 0} \gamma^k c_{[t:t+k-1]} \rho_{t+k} \delta_{t+k}^{DR}],$$

where $\delta_t^{DR} \overset{def}{=} r_t + \gamma V(s_{t+1}) - Q(s_t, a_t)$ is one-step Doubly Robust error, $\rho_t \overset{def}{=} \min\{\frac{\pi_t}{\mu_t}, \bar{\rho}\}$ and $c_t \overset{def}{=} \min\{\frac{\pi_t}{\mu_t}, \bar{c}\}$ are clipped per-step importance sampling, $c_{[t:t+k]} \overset{def}{=} \prod_{i=0}^{k} c_{t+i}$.

With one step Bellman equation, we estimate Q by

$$\begin{aligned} Q_{DR}^{\tilde{\pi}}(s_t, a_t) &\overset{def}{=} \mathbb{E}_{s_{t+1}, r_t \sim p(\cdot,\cdot|s_t,a_t)}[r_t + \gamma V_{DR}^{\tilde{\pi}}(s_{t+1})] \\ &= \mathbb{E}_\mu[Q(s_t, a_t) + \sum_{k\geq 0} \gamma^k c_{[t+1:t+k-1]} \tilde{\rho}_{t,k} \delta_{t+k}^{DR}], \end{aligned}$$

where $\tilde{\rho}_{t,k} = 1_{\{k=0\}} + 1_{\{k>0\}} \rho_{t+k}$.

Theorem 2. *Define* $\bar{A} = A - \mathbb{E}_\pi[A]$, $Q = \bar{A} + sg(V)$,

$$\begin{aligned} &\mathscr{T}(Q) \overset{def}{=} \mathbb{E}_\mu[Q(s_t, a_t) + \sum_{k\geq 0} \gamma^k c_{[t+1:t+k-1]} \tilde{\rho}_{t,k} \delta_{t+k}^{DR}], \\ &\mathscr{S}(V) \overset{def}{=} \mathbb{E}_\mu[V(s_t) + \sum_{k\geq 0} \gamma^k c_{[t:t+k-1]} \rho_{t,k} \delta_{t+k}^{DR}], \\ &\mathscr{U}(Q, V) = (\mathscr{T}(Q) - \mathbb{E}_\pi[Q] + \mathscr{S}(V), \mathscr{S}(V)), \\ &\mathscr{U}^{(n)}(Q, V) = \mathscr{U}(\mathscr{U}^{(n-1)}(Q, V)), \end{aligned}$$

then $\mathscr{U}^{(n)}(Q, V) \to (Q^{\tilde{\pi}}, V^{\tilde{\pi}})$ *that corresponds to*

$$\tilde{\pi}(a|s) = \frac{\min\{\bar{\rho}\mu(a|s), \pi(a|s)\}}{\sum_{b\in\mathcal{A}} \min\{\bar{\rho}\mu(b|s), \pi(b|s)\}}.$$

as $n \to +\infty$.

Proof. See Appendix C, Theorem C.1. □

Theorem 2 shows that DR-Trace is a contraction mapping and (V, Q) converges to $(V^{\tilde{\pi}}, Q^{\tilde{\pi}})$ that corresponds to

$$\tilde{\pi}(a|s) = \frac{\min\{\bar{\rho}\mu(a|s), \pi(a|s)\}}{\sum_{b\in\mathcal{A}} \min\{\bar{\rho}\mu(b|s), \pi(b|s)\}}.$$

According to our proof, DR-Trace should work similar to V-Trace and ReTrace, as the convergence rate and the limitation are same. We compare DR-Trace with V-Trace+ReTrace in Figure 6, where we replace estimation of state values by V-Trace and estimation of state-action values by ReTrace. We call V-Trace+ReTrace as No-DR-Trace for brevity. No-DR-Trace performs better on Breakout and ChopperCommand, but fails to make a breakthrough on Krull. Recalling the fact that Doubly Robust can maximally reduce the variance of Bellman error, No-DR-Trace is less stable but also potential to achieve a better performance. A conclusion cannot be made about No-DR-Trace, as this phenomenon means that No-DR-Trace is less stable than DR-Trace, but it also holds the potential to achieve a better performance.

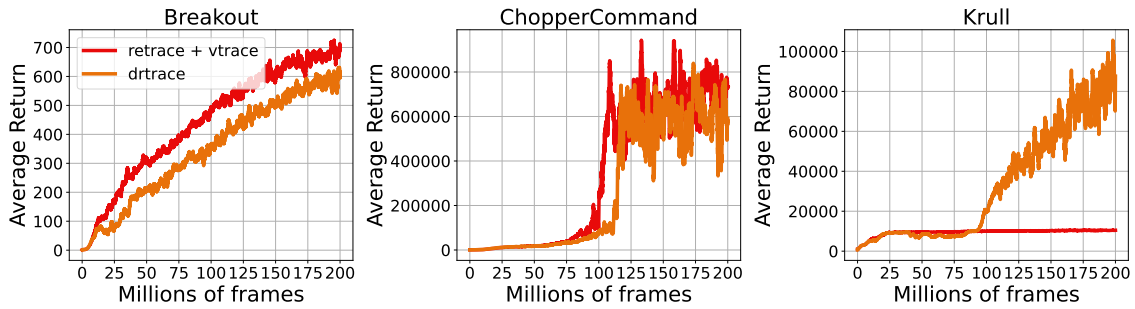

Figure 6: Ablation study for w/wo DR-Trace on Breakout, ChopperCommand and Krull.

C PROOFS

Lemma C.1. *(i) Define $\pi = softmax(A/\tau)$, then $\nabla \log \pi = (\boldsymbol{1} - \pi)\frac{\nabla A}{\tau}$. (ii) Denote sg to be stop gradient and define $\bar{A} = A - \mathbb{E}_\pi[A]$, $Q = \bar{A} + sg(V)$, then $\nabla Q = (\boldsymbol{1} - \pi)\nabla A$.*

Proof. As $Q = \bar{A} + sg(V) = A - sg(\pi) \cdot A + sg(V)$, it's obvious that $\nabla Q = (\mathbf{1} - \pi)\nabla A$.

For $\log \pi$, it's a standard derivative of cross entropy, so we have $\nabla \log \pi = (\mathbf{1} - \pi)\nabla(A/\tau) = (\mathbf{1} - \pi)\frac{\nabla A}{\tau}$. □

Lemma C.2. *Define $\bar{A} = A - \mathbb{E}_\pi[A]$, $Q = \bar{A} + sg(V), \pi = softmax(A/\tau)$, then*

$$\mathbb{E}_\pi\left[(Q - V)\nabla \log \pi\right] = -\tau \nabla \boldsymbol{H}[\pi].$$

Proof. Since

$$\pi = \exp(A/\tau)/Z,\ Z = \int_{\mathcal{A}} \exp(A/\tau),$$

we have

$$A = \tau \log \pi + \tau \log Z.$$

Based on the observation that $\mathbb{E}_\pi\left[f(s)\nabla \log \pi(\cdot|s)\right] = 0$, we have

$$\mathbb{E}_\pi\left[\mathbb{E}_\pi[A] \cdot \nabla \log \pi\right] = 0,$$

$$\mathbb{E}_\pi\left[\log Z \cdot \nabla \log \pi\right] = 0.$$

On the one hand,

$$\begin{aligned}\mathbb{E}_\pi\left[(Q - V)\nabla \log \pi\right] &= \mathbb{E}_\pi\left[A\nabla \log \pi\right] - \mathbb{E}_\pi\left[\mathbb{E}_\pi[A] \cdot \nabla \log \pi\right] \\ &= \tau\mathbb{E}_\pi\left[\log \pi \nabla \log \pi\right] + \tau\mathbb{E}_\pi\left[\log Z \cdot \nabla \log \pi\right] \\ &= \tau\mathbb{E}_\pi\left[\log \pi \nabla \log \pi\right].\end{aligned}$$

On the other hand,

$$\begin{aligned}\nabla \mathbf{H}[\pi] &= -\nabla \int_{\mathcal{A}} \pi_i \log \pi_i \\ &= -\int_{\mathcal{A}} \nabla \pi_i \cdot \log \pi_i - \int_{\mathcal{A}} \pi_i \nabla \log \pi_i \\ &= -\int_{\mathcal{A}} \pi_i \nabla \log \pi_i \cdot \log \pi_i - \int_{\mathcal{A}} \pi_i \frac{\nabla \pi_i}{\pi_i} \\ &= -\mathbb{E}_\pi \left[\log \pi \nabla \log \pi\right].\end{aligned}$$

Hence, $\mathbb{E}_\pi \left[(Q - V)\nabla \log \pi\right] = -\tau \nabla \mathbf{H}[\pi]$. □

Theorem C.1. *Define* $\bar{A} = A - \mathbb{E}_\pi[A]$, $Q = \bar{A} + sg(V)$. *Define*

$$\begin{aligned}&\mathscr{T}(Q) \stackrel{def}{=} \mathbb{E}_\mu[Q(s_t, a_t) + \sum_{k\geq 0} \gamma^k c_{[t+1:t+k-1]} \tilde{\rho}_{t,k} \delta^{DR}_{t+k}], \\ &\mathscr{S}(V) \stackrel{def}{=} \mathbb{E}_\mu[V(s_t) + \sum_{k\geq 0} \gamma^k c_{[t:t+k-1]} \rho_{t,k} \delta^{DR}_{t+k}], \\ &\mathscr{U}(Q, V) = (\mathscr{T}(Q) - \mathbb{E}_\pi[Q] + \mathscr{S}(V), \mathscr{S}(V)), \\ &\mathscr{U}^{(n)}(Q, V) = \mathscr{U}(\mathscr{U}^{(n-1)}(Q, V)),\end{aligned}$$

then $\mathscr{U}^{(n)}(Q, V) \to (Q^{\tilde{\pi}}, V^{\tilde{\pi}})$ *that corresponds to*

$$\tilde{\pi}(a|s) = \frac{\min\left\{\bar{\rho}\mu(a|s), \pi(a|s)\right\}}{\sum_{b\in\mathcal{A}} \min\left\{\bar{\rho}\mu(b|s), \pi(b|s)\right\}}.$$

as $n \to +\infty$.

Remark. $\mathscr{T}(Q) - \mathbb{E}_\pi[Q] + \mathscr{S}(V)$ is **exactly** how Q is updated at training time. Since $Q = \bar{A} + sg(V)$, if we apply gradient ascent on Q and V in directions $\nabla L_Q(\theta)$ and $\nabla L_V(\theta)$ respectively, change of Q comes from two aspects. One comes from $\nabla L_Q(\theta)$, which changes A, the other comes from $\nabla L_V(\theta)$, which changes V. Because the gradient of V is stopped when estimating Q, the latter is captured by "minus old baseline, add new baseline", which is $-\mathbb{E}_\pi[Q] + \mathscr{S}(V)$ in Theorem C.1.

Proof. Define

$$\begin{aligned}\widetilde{\mathscr{T}}(Q) &= -\mathbb{E}_\pi[Q] + \mathscr{T}(Q), \\ \widetilde{\mathscr{U}}(Q, V) &= (\widetilde{\mathscr{T}}(Q), \mathscr{S}(V)), \\ \widetilde{\mathscr{U}}^{(n)}(Q, V) &= \widetilde{\mathscr{U}}(\widetilde{\mathscr{U}}^{(n-1)}(Q, V)).\end{aligned}$$

By Lemma C.3, $\widetilde{\mathscr{T}}^{(n)}(Q)$ converges to some A^* as $n \to \infty$. This process will not influence the estimation of V as the gradient of V is stopped when estimating Q. According to the proof, A^* does not depend on V.
By Lemma C.4, $\mathscr{S}^{(n)}(V)$ converges to some V^* as $n \to \infty$.
Hence, we have

$$\widetilde{\mathscr{U}}^{(n)}(Q, V) \to (A^*, V^*) \ \ as \ \ n \to +\infty.$$

By definition,

$$\mathscr{U}(Q, V) = (\widetilde{\mathscr{T}}(Q) + \mathscr{S}(V), \mathscr{S}(V)),$$

we can regard $\widetilde{\mathscr{T}}(Q)+\mathscr{S}(V)$ as Q and regard $\mathscr{S}(V)$ as V, then

$$\begin{aligned}\mathscr{U}^{(2)}(Q,V) &= \mathscr{U}(\widetilde{\mathscr{T}}(Q)+\mathscr{S}(V),\mathscr{S}(V))\\ &= (\mathscr{T}(\widetilde{\mathscr{T}}(Q)+\mathscr{S}(V))-\mathscr{S}(V)+\mathscr{S}^{(2)}(V),\mathscr{S}^{(2)}(V))\\ &= (\widetilde{\mathscr{T}}^{(2)}(Q)+\mathscr{S}^{(2)}(V),\mathscr{S}^{(2)}(V)).\end{aligned}$$

By induction,

$$\begin{aligned}\mathscr{U}^{(n)}(Q,V) &= (\widetilde{\mathscr{T}}^{(n)}(Q)+\mathscr{S}^{(n)}(V),\mathscr{S}^{(n)}(V))\\ &\to (A^*+V^*,V^*)\ \ as\ \ n\to+\infty.\end{aligned}$$

Same as (Espeholt et al., 2018),

$$\tilde{\pi}(a|s)=\frac{\min\{\bar{\rho}\mu(a|s),\pi(a|s)\}}{\sum_{b\in\mathcal{A}}\min\{\bar{\rho}\mu(b|s),\pi(b|s)\}}.$$

is the policy s.t. the Bellman equation holds, which is

$$\mathbb{E}_\mu[\rho_t(r_t+\gamma V_{t+1}-V_t)|\mathscr{F}_t]=0,$$

and $\mathscr{U}(Q^{\tilde{\pi}},V^{\tilde{\pi}})=(Q^{\tilde{\pi}},V^{\tilde{\pi}})$.
So we have $(A^*+V^*,V^*)=(Q^{\tilde{\pi}},V^{\tilde{\pi}})$. □

Lemma C.3. *Define $\bar{A}=A-\mathbb{E}_\pi[A]$, $Q=\bar{A}+sg(V)$, then operator*

$$\mathscr{T}(Q)\overset{def}{=}\mathbb{E}_\mu[Q(s_t,a_t)+\sum_{k\geq 0}\gamma^k c_{[t+1:t+k-1]}\tilde{\rho}_{t,k}\delta^{DR}_{t+k}]$$

is a contraction mapping w.r.t. Q.

Remark. Note that $\mathscr{T}(Q)$ is exactly equation B.

Since $Q=A+sg(V)$, the gradient of V is stopped when estimating Q, updating Q will not change V, which is equivalent to updating A. Without loss of generality, we assume V is fixed as V^* in the proof.

Proof. $\bar{A}=A-\mathbb{E}_\pi[A]$ shows $\mathbb{E}_\pi[\bar{A}]=0$, which guarantees that no matter how we update A, we always have $\mathbb{E}_\pi[Q]=V^*$.

Based on above observations, define

$$\widetilde{\mathscr{T}}(Q)\overset{def}{=}-\mathbb{E}_\pi[Q]+\mathscr{T}(Q).$$

It's obvious that we only need to prove $\widetilde{\mathscr{T}}(Q)$ is a contraction mapping.

For brevity, we denote

$$Q_t=Q(s_t,a_t),A_t=A(s_t,a_t),V^*_t=V^*(s_t).$$

Noticing that $\tilde{\rho}_{t,0}=1$, let $\mathscr{F}$ represent filtration, we can rewrite $\widetilde{\mathscr{T}}$ as

$$\begin{aligned}\widetilde{\mathscr{T}}(Q) &= \mathbb{E}_\mu[A_t+\sum_{k\geq 0}\gamma^k c_{[t+1:t+k-1]}\tilde{\rho}_{t,k}\delta^{DR}_{t+k}]\\ &= \mathbb{E}_\mu[-V^*_t+\sum_{k\geq 0}\gamma^k c_{[t+1:t+k-1]}\tilde{\rho}_{t,k}r_{t+k}+\sum_{k\geq 0}\gamma^{k+1}c_{[t+1:t+k-1]}\Delta_k],\end{aligned}\tag{9}$$

where

$$\Delta_k = \mathbb{E}_\mu \left[\tilde{\rho}_{t,k} V^*_{t+k+1} - c_{t+k} \tilde{\rho}_{t,k+1} Q_{t+k+1} | \mathscr{F}_{t+k} \right]. \tag{10}$$

By definition of Q,

$$\mathbb{E}_\mu[V^*_{t+k+1}|\mathscr{F}_{t+k}] = \mathbb{E}_\mu[\mathbb{E}_\pi[Q_{t+k+1}|\mathscr{F}_{t+k+1}]|\mathscr{F}_{t+k}],$$

we can rewrite equation 10 as

$$\Delta_k = \mathbb{E}_\mu[(\tilde{\rho}_{t,k} \frac{\pi_{t+k+1}}{\mu_{t+k+1}} - c_{t+k}\tilde{\rho}_{t,k+1}) Q_{t+k+1} | \mathscr{F}_{t+k}]. \tag{11}$$

For any $Q_1 = A_1 + sg(V^*)$, $Q_2 = A_2 + sg(V^*)$, since

$$\mathbb{E}_\mu[(\tilde{\rho}_{t,k} \frac{\pi_{t+k+1}}{\mu_{t+k+1}} - c_{t+k}\tilde{\rho}_{t,k+1}) | \mathscr{F}_{t+k}] \geq 0,$$

by equation 9 equation 11, we have

$$||\widetilde{\mathscr{T}}(Q_1) - \widetilde{\mathscr{T}}(Q_2)|| \leq \mathcal{C}||Q_1 - Q_2||,$$

where

$$\begin{aligned}
\mathcal{C} &= \mathbb{E}_\mu[\sum_{k\geq 0} \gamma^{k+1} c_{[t+1:t+k-1]} (\tilde{\rho}_{t,k} \frac{\pi_{t+k+1}}{\mu_{t+k+1}} - c_{t+k}\tilde{\rho}_{t,k+1})] \\
&= \mathbb{E}_\mu[1 - 1 + \sum_{k\geq 0} \gamma^{k+1} c_{[t+1:t+k-1]} (\tilde{\rho}_{t,k} - c_{t+k}\tilde{\rho}_{t,k+1})] \\
&= 1 - (1-\gamma)\mathbb{E}_\mu[\sum_{k\geq 0} \gamma^k c_{[t+1:t+k-1]} \tilde{\rho}_{t,k}] \\
&\leq 1 - (1-\gamma) < 1.
\end{aligned}$$

Hence, $\widetilde{\mathscr{T}}(Q)$ is a contraction mapping and converges to some fixed function, which we denote as A^*. So $\mathscr{T}(Q)$ is also a contraction mapping and converges to $A^* + V^*$. □

Lemma C.4. *Define $Q = A + sg(V)$ with $\mathbb{E}_\pi[A] = 0$, then operator*

$$\mathscr{S}(V) \stackrel{def}{=} \mathbb{E}_\mu[V(s_t) + \sum_{k\geq 0} \gamma^k c_{[t:t+k-1]} \rho_{t,k} \delta^{DR}_{t+k}]$$

is a contraction mapping w.r.t. V.

Remark. Note that $\mathscr{S}(V)$ is exactly equation B.

Proof. Same as Lemma C.3, we can get

$$\Delta_k = \mathbb{E}_\mu \left[(\rho_{t+k} - c_{t+k}\rho_{t+k+1}) V_{t+k+1} - c_{t+k}\rho_{t+k+1} A^*_{t+k+1} | \mathscr{F}_{t+k} \right],$$

so we have

$$\Delta^1_k - \Delta^2_k = \mathbb{E}_\mu \left[(\rho_{t+k} - c_{t+k}\rho_{t+k+1}) \cdot (V^1_{t+k+1} - V^2_{t+k+1}) | \mathscr{F}_{t+k} \right].$$

The remaining proof is identical to (Espeholt et al., 2018)'s. □

D HYPERPARAMETERS

Our python packages are shown in Table 7.

Package	Version
ale-py	0.6.0.dev20200207
gym	0.19.0
tensorflow	1.15.2
opencv-python	4.1.2.30
opencv-contrib-python	4.4.0.46

Table 7: Versions for python packages among all experiments.

All experiments follow the shared hyperparameters as in Table 8. The specific hyperparameters for PPO, R2D2 and CASA+DR-Trace are shown in Table 9, Table 10 and Table 11. The only exceptions are V-loss scaling, Q-loss scaling and π-loss scaling, which may be zero depending on some specific ablation settings. We will state these three hyperparameters every time in all experiments.

Parameter	Value
Atari Version	NoFrameskip-v4
Atari Wrapper	gym.wrappers.atari_preprocessing
Image Size	(84, 84)
Grayscale	Yes
Num. Action Repeats	4
Num. Frame Stacks	4
Action Space	Full
End of Episode When Life Lost	No
Num. States	200M
Num. Environments	160
Random No-ops	30
Burn-in	40
Seq-length	80
Burn-in Stored Recurrent State	Yes
Bootstrap	Yes
Batch size	64
Backbone	IMPALA,deep
LSTM Units	256
Optimizer	Adam Weight Decay
Weight Decay Rate	0.01
Weight Decay Schedule	Anneal linearly to 0
Learning Rate	5e-4
Warmup Steps	4000
Learning Rate Schedule	Anneal linearly to 0
AdamW β_1	0.9
AdamW β_2	0.98
AdamW ϵ	1e-6
AdamW Clip Norm	50.0
Learner Push Model Every n Steps	25
Actor Pull Model Every n Steps	64

Table 8: Configurations for shared hyperparameters among all experiments.

Parameter	Value
Sample Reuse	1
Reward Shape	$\text{clip}(r, 0, 1)$
Discount (γ)	0.995
V-loss Scaling (α_1)	0.5
Q-loss Scaling (α_2)	1.0
π-loss Scaling (α_3)	1.0
PPO clip ϵ	0.2
GAE λ	0.8
Temperature (τ)	0.1

Table 9: Hyperparameter configurations for PPO.

Parameter	Value
Sample Reuse	2
Target Shape	$Q_t^{\tilde{\pi}} = h(\sum_{i=0}^{n-1} \gamma^i r_{t+i} + \gamma^n h^{-1}(\text{Double}(Q_{t+n})))$
Target Shape Function h	$h(x) = \text{sign}(x) \cdot (\sqrt{\lvert x \rvert + 1} - 1) + 10^{-3}x$
Bootstrap Length n	5
ϵ-greedy	$\epsilon \sim 0.4^{\text{uniform}(1,8)}$
PER Sample Temperature α	0.9
PER Buffer Size	400000
Discount (γ)	0.997
V-loss Scaling (α_1)	0.5
Q-loss Scaling (α_2)	1.0
π-loss Scaling (α_3)	1.0
Temperature (τ)	0.1

Table 10: Hyperparameter configurations for R2D2.

Parameter	Value
Sample Reuse	2
Reward Shape	$\log(\lvert r \rvert + 1.0) \cdot (2 \cdot 1_{\{r \geq 0\}} - 1_{\{r < 0\}})$
Discount (γ)	0.997
V-loss Scaling (α_1)	1.0
Q-loss Scaling (α_2)	10.0
π-loss Scaling (α_3)	10.0
Temperature (τ)	1.0
Importance Sampling Clip $\bar{c}$	1.05
Importance Sampling Clip $\bar{\rho}$	1.05

Table 11: Hyperparameter configurations for CASA + DR-Trace.

E EVALUATION OF CASA ON ATARI GAMES

Random scores and average human's scores are from (Badia et al., 2020). Human World Records (HWR) are from (Toromanoff et al., 2019). Rainbow's scores are from (Hessel et al., 2017). IMPALA's scores are from (Espeholt et al., 2018). LASER's scores are from (Schmitt et al., 2020), no sweep at 200M.

Games	RND	HUMAN	RAINBOW	HNS(%)	IMPALA	HNS(%)	LASER	HNS(%)	CASA	HNS(%)
Scale			200M		200M		200M		200M	
alien	227.8	7127.8	9491.7	134.26	15962.1	228.03	**35565.9**	**512.15**	26137	375.50
amidar	5.8	1719.5	**5131.2**	**299.08**	1554.79	90.39	1829.2	106.4	560	32.34
assault	222.4	742	14198.5	2689.78	19148.47	3642.43	**21560.4**	**4106.62**	16228	3080.37
asterix	210	8503.3	**428200**	**5160.67**	300732	3623.67	240090	2892.46	213580	2572.80
asteroids	719	47388.7	2712.8	4.27	108590.05	231.14	**213025**	**454.91**	80339	170.60
atlantis	12850	29028.1	826660	5030.32	849967.5	5174.39	841200	5120.19	**3211600**	**19772.10**
bank heist	14.2	753.1	**1358**	**181.86**	1223.15	163.61	569.4	75.14	895.3	119.24
battle zone	236	37187.5	62010	167.18	20885	55.88	64953.3	175.14	**91269**	**246.36**
beam rider	363.9	16926.5	16850.2	99.54	32463.47	193.81	**90881.6**	**546.52**	57456	344.70
berzerk	123.7	2630.4	2545.6	96.62	1852.7	68.98	**25579.5**	**1015.51**	1648	60.81
bowling	23.1	160.7	30	5.01	59.92	26.76	48.3	18.31	**162.4**	**101.24**
boxing	0.1	12.1	99.6	829.17	99.96	832.17	**100**	**832.5**	98.3	818.33
breakout	1.7	30.5	417.5	1443.75	**787.34**	**2727.92**	747.9	2590.97	624.3	2161.81
centipede	2090.9	12017	8167.3	61.22	11049.75	90.26	**292792**	**2928.65**	102600	1012.57
chopper command	811	7387.8	16654	240.89	28255	417.29	**761699**	**11569.27**	616690	9364.42
crazy climber	10780.5	36829.4	**168788.5**	**630.80**	136950	503.69	167820	626.93	161250	600.70
defender	2874.5	18688.9	55105	330.27	185203	1152.93	336953	2112.50	**421600**	**2647.75**
demon attack	152.1	1971	111185	6104.40	132826.98	7294.24	133530	7332.89	**291590**	**16022.76**
double dunk	-18.6	-16.4	-0.3	831.82	-0.33	830.45	14	1481.82	**20.25**	**1765.91**
enduro	0	860.5	2125.9	247.05	0	0.00	0	0.00	**10019**	**1164.32**
fishing derby	-91.7	-38.8	31.3	232.51	44.85	258.13	45.2	258.79	**53.24**	**273.99**
freeway	0	29.6	**34**	**114.86**	0	0.00	0	0.00	3.46	11.69
frostbite	65.2	4334.7	**9590.5**	**223.10**	317.75	5.92	5083.5	117.54	1583	35.55
gopher	257.6	2412.5	70354.6	3252.91	66782.3	3087.14	114820.7	5316.40	**188680**	**8743.90**
gravitar	173	3351.4	1419.3	39.21	359.5	5.87	1106.2	29.36	**4311**	**130.19**
hero	1027	30826.4	**55887.4**	**184.10**	33730.55	109.75	31628.7	102.69	24236	77.88
ice hockey	-11.2	0.9	1.1	101.65	3.48	121.32	**17.4**	**236.36**	1.56	105.45
jamesbond	29	302.8	19809	72.24	601.5	209.09	**37999.8**	**13868.08**	12468	4543.10
kangaroo	52	3035	**14637.5**	**488.05**	1632	52.97	14308	477.91	5399	179.25
krull	1598	2665.5	8741.5	669.18	8147.4	613.53	9387.5	729.70	**64347**	**5878.13**
kung fu master	258.5	22736.3	52181	230.99	43375.5	191.82	**607443**	**2701.26**	124630.1	553.31
montezuma revenge	0	**4753.3**	384	8.08	0	0.00	0.3	0.01	2488.4	52.35
ms pacman	307.3	6951.6	5380.4	76.35	7342.32	105.88	6565.5	94.19	**7579**	**109.44**
name this game	2292.3	8049	13136	188.37	21537.2	334.30	26219.5	415.64	**32098**	**517.76**
phoenix	761.5	7242.6	108529	1662.80	210996.45	3243.82	**519304**	**8000.84**	498590	7681.23
pitfall	-229.4	**6463.7**	0	3.43	-1.66	3.40	-0.6	3.42	-17.8	3.16
pong	-20.7	14.6	20.9	117.85	20.98	118.07	**21**	**118.13**	20.39	116.40
private eye	24.9	**69571.3**	4234	6.05	98.5	0.11	96.3	0.10	134.1	0.16
qbert	163.9	13455.0	33817.5	253.20	**351200.12**	**2641.14**	21449.6	160.15	27371	204.70
riverraid	1338.5	17118.0	22920.8	136.77	29608.05	179.15	**40362.7**	**247.31**	11182	62.38
road runner	11.5	7845	62041	791.85	57121	729.04	45289	578.00	**251360**	**3208.64**
robotank	2.2	11.9	61.4	610.31	12.96	110.93	**62.1**	**617.53**	10.44	84.95
seaquest	68.4	**42054.7**	15898.9	37.70	1753.2	4.01	2890.3	6.72	11862	28.09
skiing	-17098	**-4336.9**	-12957.8	32.44	-10180.38	54.21	-29968.4	-100.86	-12730	34.23
solaris	1236.3	**12326.7**	3560.3	20.96	2365	10.18	2273.5	9.35	2319	9.76
space invaders	148	1668.7	18789	1225.82	43595.78	2857.09	**51037.4**	**3346.45**	3031	189.58
star gunner	664	10250	127029	1318.22	200625	2085.97	321528	3347.21	**337150**	**3510.18**
surround	-10	6.5	**9.7**	**119.39**	7.56	106.42	8.4	111.52	-10	0.00
tennis	-23.8	-8.3	0	153.55	0.55	157.10	**12.2**	**232.26**	-21.05	17.74
time pilot	3568	5229.2	12926	563.36	48481.5	2703.84	**105316**	**6125.34**	84341	4862.62
tutankham	11.4	167.6	241	146.99	292.11	179.71	278.9	171.25	**381**	**236.62**
up n down	533.4	11693.2	125755	1122.08	332546.75	2975.08	345727	3093.19	**416020**	**3723.06**
venture	0	**1187.5**	5.5	0.46	0	0.00	0	0.00	0	0.00
video pinball	0	17667.9	533936.5	3022.07	**572898.27**	**3242.59**	511835	2896.98	297920	1686.22
wizard of wor	563.5	4756.5	17862.5	412.57	9157.5	204.96	**29059.3**	**679.60**	26008	606.83
yars revenge	3092.9	54576.9	102557	193.19	84231.14	157.60	**166292.3**	**316.99**	118730	224.61
zaxxon	32.5	9173.3	22209.5	242.62	32935.5	359.96	41118	449.47	**46070.8**	**503.66**
MEAN HNS(%)	0.00	100.00		873.97		957.34		1741.36		1941.08
MEDIAN HNS(%)	0.00	100.00		230.99		191.82		454.91		246.36

Games	RND	HWR	RAINBOW	SABER(%)	IMPALA	SABER(%)	LASER	SABER(%)	CASA	SABER(%)
Scale			200M		200M		200M		200M	
alien	227.8	**251916**	9491.7	3.68	15962.1	6.25	976.51	14.04	26137	10.29
amidar	5.8	**104159**	5131.2	4.92	1554.79	1.49	1829.2	1.75	560	0.53
assault	222.4	8647	14198.5	165.90	19148.47	200.00	**21560.4**	**200.00**	16228	189.99
asterix	210	**1000000**	428200	42.81	300732	30.06	240090	23.99	213580	21.34
asteroids	719	**10506650**	2712.8	0.02	108590.05	1.03	213025	2.02	80339	0.76
atlantis	12850	**10604840**	826660	7.68	849967.5	7.90	841200	7.82	3211600	30.20
bank heist	14.2	**82058**	1358	1.64	1223.15	1.47	569.4	0.68	895.3	1.07
battle zone	236	**801000**	62010	7.71	20885	2.58	64953.3	8.08	91269	11.37
beam rider	363.9	**999999**	16850.2	1.65	32463.47	3.21	90881.6	9.06	57456	5.71
berzerk	123.7	**1057940**	2545.6	0.23	1852.7	0.16	25579.5	2.41	1648	0.14
bowling	23.1	**300**	30	2.49	59.92	13.30	48.3	9.10	162.4	50.31
boxing	0.1	**100**	99.6	99.60	99.96	99.96	**100**	**100.00**	98.3	98.3
breakout	1.7	**864**	417.5	48.22	787.34	91.11	747.9	86.54	624.3	72.20
centipede	2090.9	**1301709**	8167.3	0.47	11049.75	0.69	292792	22.37	102600	7.73
chopper command	811	**999999**	16654	1.59	28255	2.75	761699	76.15	616690	61.64
crazy climber	10780.5	**219900**	168788.5	75.56	136950	60.33	167820	75.10	161250	71.95
defender	2874.5	**6010500**	55105	0.87	185203	3.03	336953	5.56	421600	6.97
demon attack	152.1	**1556345**	111185	7.13	132826.98	8.53	133530	8.57	291590	18.73
double dunk	-18.6	**21**	-0.3	46.21	-0.33	46.14	14	82.32	20.25	98.11
enduro	0	9500	2125.9	22.38	0	0.00	0	0.00	**10019**	**105.46**
fishing derby	-91.7	**71**	31.3	75.60	44.85	83.93	45.2	84.14	53.24	89.08
freeway	0	**38**	34	89.47	0	0.00	0	0.00	3.46	9.11
frostbite	65.2	**454830**	9590.5	2.09	317.75	0.06	5083.5	1.10	1583	0.33
gopher	257.6	**355040**	70354.6	19.76	66782.3	18.75	114820.7	32.29	188680	53.11
gravitar	173	**162850**	1419.3	0.77	359.5	0.11	1106.2	0.57	4311	2.54
hero	1027	**1000000**	55887.4	5.49	33730.55	3.27	31628.7	3.06	24236	2.32
ice hockey	-11.2	**36**	1.1	26.06	3.48	31.10	17.4	60.59	1.56	27.03
jamesbond	29	**45550**	19809	43.45	601.5	1.26	37999.8	83.41	12468	27.33
kangaroo	52	**1424600**	14637.5	1.02	1632	0.11	14308	1.00	5399	0.38
krull	1598	**104100**	8741.5	6.97	8147.4	6.39	9387.5	7.60	64347	61.22
kung fu master	258.5	**1000000**	52181	5.19	43375.5	4.31	607443	60.73	124630.1	12.44
montezuma revenge	0	**1219200**	384	0.03	0	0.00	0.3	0.00	2488.4	0.20
ms pacman	307.3	**290090**	5380.4	1.75	7342.32	2.43	6565.5	2.16	7579	2.51
name this game	2292.3	25220	13136	47.30	21537.2	83.94	26219.5	104.36	**32098**	**130.00**
phoenix	761.5	**4014440**	108529	2.69	210996.45	5.24	519304	12.92	498590	12.40
pitfall	-229.4	**114000**	0	0.20	-1.66	0.20	-0.6	0.20	-17.8	0.19
pong	-20.7	**21**	20.9	99.76	20.98	99.95	**21**	**100.00**	20.39	98.54
private eye	24.9	**101800**	4234	4.14	98.5	0.07	96.3	0.07	134.1	0.11
qbert	163.9	**2400000**	33817.5	1.40	351200.12	14.63	21449.6	0.89	27371	1.13
riverraid	1338.5	**1000000**	22920.8	2.16	29608.05	2.83	40362.7	3.91	11182	0.99
road runner	11.5	**2038100**	62041	3.04	57121	2.80	45289	2.22	251360	12.33
robotank	2.2	**76**	61.4	80.22	12.96	14.58	62.1	81.17	10.44	11.17
seaquest	68.4	**999999**	15898.9	1.58	1753.2	0.17	2890.3	0.28	11862	1.18
skiing	-17098	**-3272**	-12957.8	29.95	-10180.38	50.03	-29968.4	-93.09	-12730	31.59
solaris	1236.3	**111420**	3560.3	2.11	2365	1.02	2273.5	0.94	2319	0.98
space invaders	148	**621535**	18789	3.00	43595.78	6.99	51037.4	8.19	3031	0.46
star gunner	664	77400	127029	164.67	200625	200.00	321528	200.00	**337150**	**200.00**
surround	-10	9.6	**9.7**	**100.51**	7.56	89.59	8.4	93.88	-10	0.00
tennis	-23.8	**21**	0	53.13	0.55	54.35	12.2	80.36	-21.05	6.14
time pilot	3568	65300	12926	15.16	48481.5	72.76	**105316**	**164.82**	84341	130.84
tutankham	11.4	**5384**	241	4.27	292.11	5.22	278.9	4.98	381	6.88
up n down	533.4	82840	125755	152.14	332546.75	200.00	345727	200.00	**416020**	**200.00**
venture	0	**38900**	5.5	0.01	0	0.00	0	0.00	0	0.00
video pinball	0	**89218328**	533936.5	0.60	572898.27	0.64	511835	0.57	297920	0.33
wizard of wor	563.5	**395300**	17862.5	4.38	9157.5	2.18	29059.3	7.22	26008	6.45
yars revenge	3092.9	**15000105**	102557	0.66	84231.14	0.54	166292.3	1.09	118730	0.77
zaxxon	32.5	**83700**	22209.5	26.51	32935.5	39.33	41118	49.11	46070.8	55.03
MEAN SABER(%)	0.00	100.00		28.39		29.45		36.78		36.10
MEDIAN SABER(%)	0.00	100.00		4.92		4.31		8.08		10.29

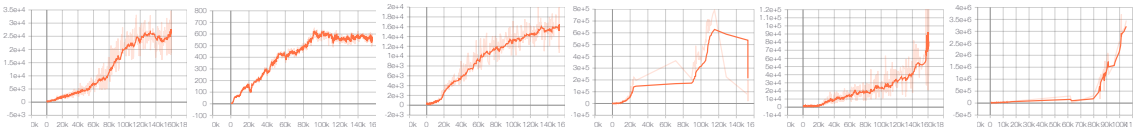

(1.) Alien (2.) Amidar (3.) Assault (4.) Asterix (5.) Asteroids (6.) Atlantis

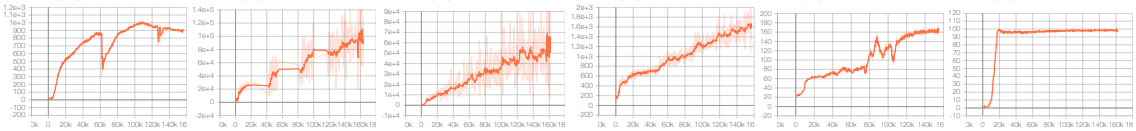

(7.) BankHeist (8.) BattleZone (9.) BeamRider (10.) Berzerk (11.) Bowling (12.) Boxing

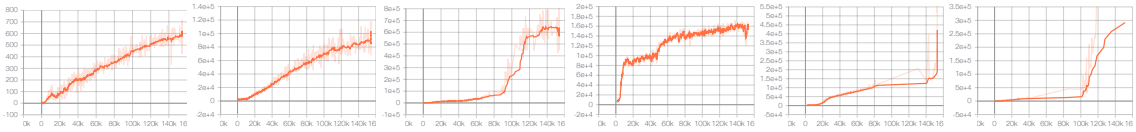

(13.) Breakout (14.) Centipede (15.) ChopperCommand (16.) CrazyClimber (17.) Defender (18.) DemonAttack

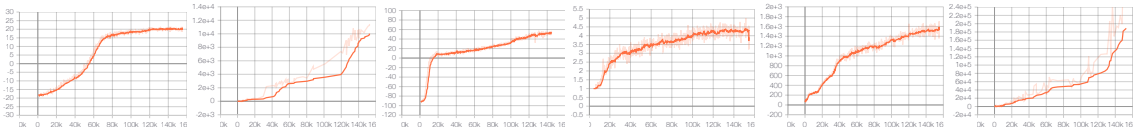

(19.) DoubleDunk (20.) Enduro (21.) FishingDerby (22.) Freeway (23.) Frostbite (24.) Gopher

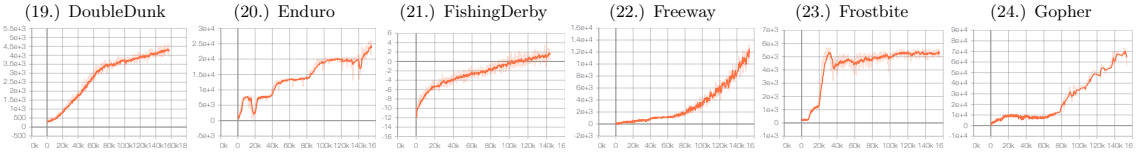

(25.) Gravitar (26.) Hero (27.) IceHockey (28.) Jamesbond (29.) Kangaroo (30.) Krull

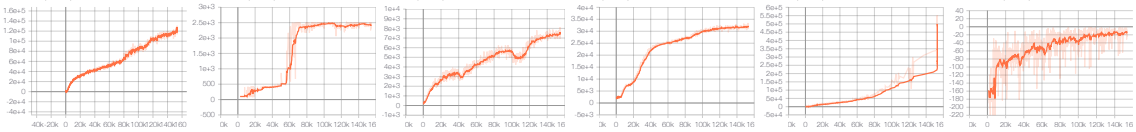

(31.) KungFuMaster (32.) MontezumaRevenge (33.) MsPacman (34.) NameThisGame (35.) Phoenix (36.) Pitfall

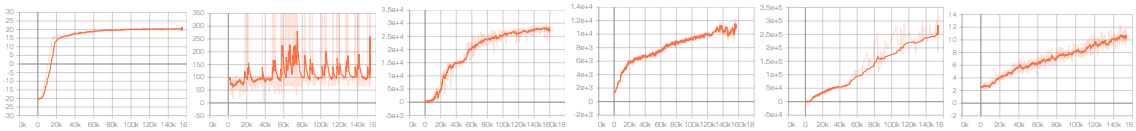

(37.) Pong (38.) PrivateEye (39.) Qbert (40.) Riverraid (41.) RoadRunner (42.) Robotank

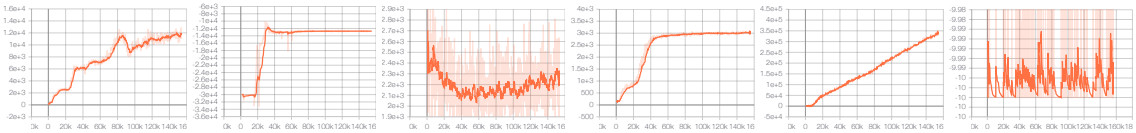

(43.) Seaquest (44.) Skiing (45.) Solaris (46.) SpaceInvaders (47.) StarGunner (48.) Surround

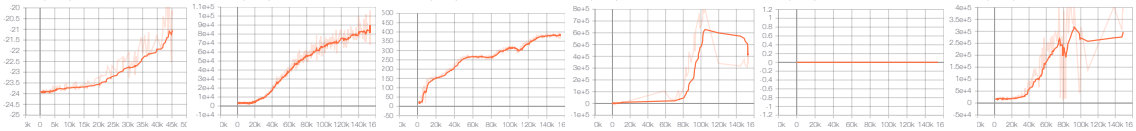

(49.) Tennis (50.) TimePilot (51.) Tutankham (52.) UpNDown (53.) Venture (54.) VideoPinball

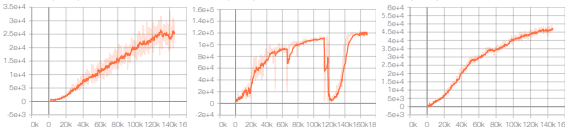

(55.) WizardOfWor (56.) YarsRevenge (57.) Zaxxon